Acta Scientiarum

http://periodicos.uem.br/ojs/acta
ISSN on-line: 1807-8664
Doi: 10.4025/actascitechnol.v40i1.30792

MECHANICAL ENGINEERING

Characteristics of interstitial fluid flow along with blood flow inside a cylindrical tumor: a numerical simulation

Mostafa Zakariapour[1*], Mohammad Hossein Hamedi[2] and Nasser Fatouraee[3]

*[1]Department of Mechanical Engineering, Ramsar Branch, Islamic Azad University, Ramsar, Iran, 46919-66434. [2]Department of Mechanical Engineering, K.N.T. University of Technology, Pardis Street, Tehran, Iran. [3]Department of Biomedical Engineering, Amirkabir University of Technology, Hafez Street, Amirkabir, Tehran, Iran. *Author for correspondence. E-mail: mzakariapour@yahoo.com*

ABSTRACT. A numerical simulation of interstitial fluid flow and blood flow is developed to a tissue containing a two-dimensional cylindrical tumor. The tumor is assumed to be a rigid porous medium with a necrotic core, interstitial fluid and two capillaries with an arterial pressure input and a venous pressure output. The interstitial fluid pressure, velocity, blood pressure as well as velocity are calculated using finite difference method. Results show that the interstitial pressure has a maximum value at the center of the tumor and decreases by moving toward the first capillary. The reduction continues between two capillaries, and interstitial pressure finally decreases in the direction of the tumor perimeter.

Keywords: interstitial fluid, porous media, finite difference, blood, cylindrical tumor.

Características do fluxo de fluido intersticial junto com o fluxo sanguíneo no interior de um tumor cilíndrico: uma simulação numérica

RESUMO. Neste trabalho desenvolveu-se uma simulação numérica de fluxo de fluido intersticial e fluxo sanguíneo para um tecido contendo um tumor cilíndrico bidimensional. Considerou-se o tumor como um meio poroso rígido com núcleo necrótico, fluido intersticial e dois capilares com entrada de pressão arterial e saída de pressão venosa. A pressão do fluido intersticial, a velocidade, a pressão sanguínea e a velocidade foram calculadas usando o método da diferença finita. Os resultados mostraram que a pressão intersticial apresentou um valor máximo no centro do tumor e diminuiu movendo-se em direção ao primeiro capilar. Observou-se que a redução continua entre os dois capilares, e finalmente a pressão intersticial diminuiu na direção do perímetro do tumor.

Palavras-chave: fluido intersticial, meio poroso, diferenças finitas, sangue, tumor cilíndrico.

Introduction

Cancer is a sophisticated illness which contains phenomena across different scales from the molecular genetic level to the tissue as a whole. Most of the cancers are made of solid tumors. Cancerous cells of solid tumors have under gone mutations all of which combined lead to cancer (Welter & Rieger, 2013). Chemo (drug/chemical) therapy, radiation, surgical ablation and hyperthermia methods are options generally available in cancer treatment (Attaluri, Ma, Qiu, Li, & Zhu, 2011). Although the most important cancer treatment is surgical removal of such tumors, the key to a successful cure often involves efficient delivery of anticancer drugs to the tumor site after the surgery. But drug delivery has many problems such as two factors that inhibit the effective delivery of drugs within tumors: non-uniform blood supply and non-uniform interstitial pressure distribution (Jain & Baxter, 1988; Jain, 1988).

Drugs inhabit most readily in areas with the best blood supply. In solid tumors, these areas are near to the vessels and tumor's peripheral space; however, 90% of a tumor receives no drug, it means that treated tumors tend to grow, because only their outer walls have been killed by the drugs (Goldacre & Sylven, 1962; Powe et al., 1984; Shah, Gallagher, & Sands, 1985; Blakeslee, 1989). Two techniques are currently used to deliver drugs to a tumor. The first, is to deliver drugs to the tumor vasculature through its supplying artery; however, this method is not effective for poorly perfused tumors. Furthermore, for a tumor with an irregular shape, inadequate drugs distribution may cause under-dosage of treatment in the tumor. The second approach, is to directly inject drugs into the extracellular space in tumors. Drugs diffuse inside the tissue after injection and move by interstitial fluid. Variations in the interstitial pressure reduce fluid exchange and further inhibit the movement of the drug into the

center of the tumor. Previous research has shown the drug delivery mechanism in tumors (Matsuki & Yanada, 1994).

McDougall, Anderson, Chaplain, and Sherratt (2002) simulated blood flow and drug delivery through the vascular network from a nearby parent vessel to the tumor surface via an associated capillary bed generated from their mathematical model of tumor-induced angiogenesis. Baxter and Jain, based on the theoretical framework in their 1D mathematical model, found that in addition to blood flow heterogeneities, some parameters such as interstitial fluid pressure (IFP) and interstitial fluid velocity (IFV) have important role in drugs delivery (Jain & Hartley, 1984; Baxter & Jain, 1990, 1991a). Saltzman and Radomsky (1991) developed methods for modeling drug transport in tissue in the vicinity of a continuous source by using polymers. Netti, Baxter, Boucher, Skalak, and Jain (1995) studied the effect of elevated IFP on vascular flow. In this case, the IFP was assumed constant, and the vascular pressure profile along the length of the vessels was predicted. Baish, Netti, and Jain (1997) investigated transmural coupling of fluid flow in microcirculatory network and interstitium in tumors. In this study they considered a potential source of nonuniformity in the blood flow: the enhanced fluid exchange between the vascular and interstitial space mediated by the high leakiness of tumor vessels which could lead to a coupling between vascular, transvascular and interstitial fluid flow.

Soltani & Chen (2011), Sefidgar et al. (2014) developed a mathematical model of interstitial fluid flow using a numerical element-based finite volume method for modeling the continuity equation in the porous media of spherical tumors. They introduced two new parameters: the critical tumor radius and the critical necrotic radius.

Wang and Li (1998) and Wang, Li, Teo, and Lee (1999) developed a simulation framework of drug delivery to tumors. They considered high interstitial pressure in tumors, the consequences of blood and lymphatic drainage. They compared in vitro results with numerical results. Jain and Hartley (1984), Baxter & Jain (1990, 1991) used a model of a spherical tumor that had continuously distributed vasculature inthe presence of the lymphatic system. Soltani and Chen (2012) investigated the effects of tumor shape, size and tissue transport properties on drug delivery to the solid tumors. In their study, they showed that among diffusion and convection mechanisms of drug transport, diffusion is dominant in most different tumor shapes and sizes. In the tumors in which, the convection has considerable effect, the drug concentration is larger than that of other tumors at the same time post injection. Pozrikidis (2010) and Pozrikidis and Farrow (2003) studied numerical simulation of blood and interstitial flow through a solid tumor. Their results showed that, the assumption of uniform interstitial pressure is not generally appropriate, and the effect of the interstitial hydraulic and vascular permeability on the fractional plasma leakage is considerable.

It should be mentioned that in none of these studies, the tumor with cylindrical geometry, and fluids flow (interstitial fluid and blood) in normal and tumor tissues is not considered. Therefore, in this work, a two-dimensional cylindrical geometry of a tumor with a variable necrotic region and two capillaries with a defined diameter and defined distance is considered. To obtain the interstitial fluid pressure and velocity in the tumor, blood flow pressure and velocity in the capillaries, a numerical scheme is proposed and the effects of different parameters such as necrotic radius, hydraulic conductivity and intercapillary distance (the distance between two capillaries) are investigated.

Material and methods

Proposed model

The aim of this study is to calculate the interstitial fluid pressure of a tumor using a simplified tumor vascular network. Real vascular system is comprised of arteries and veins. The blood path inside a real tumor is complicated and includes loops, trifurcations, shunts and dead ends. However, to simplify such a complex system, a cylindrical tumor with a necrotic core has been modeled in this study which there is no vessel in the necrotic core. The external part of the tumor contains two capillaries as it is shown in Figure 1. Actually, this geometry provides an interstitial flow from tumor center toward it's around. Besides, the possibility of observation of the interstitial pressure variations between capillaries is provided.

In this proposed model, the tumor has a diameter of 1 cm and the necrotic radius is variable. The capillaries diameter is 15 μm and the intercapillary distance is 100 μm (Soltani & Chen, 2012). Also the height of the tumor is 1 cm. It is considered thatthe blood flow through capillaries embedded in tumor tissue, as shown in Figure 1.

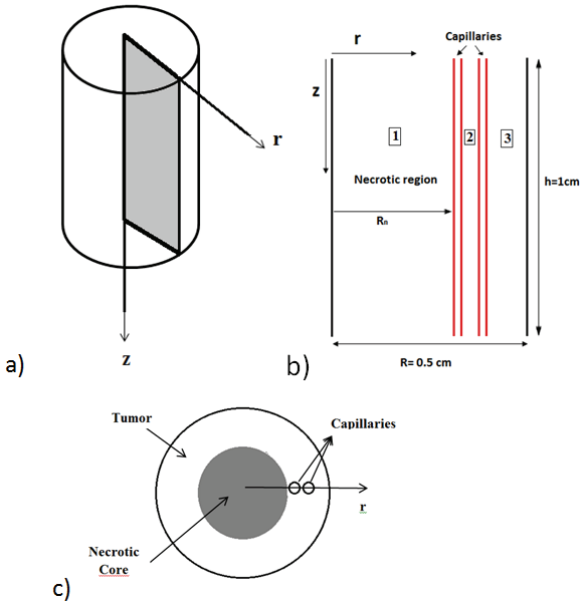

Figure 1. Geometry of tumor with capillaries; a) 2-D cylindrical tissue; b) r-z computational domain; and c) Upside view.

Mathematical model of interstitial and blood flows

The mathematical model should be accurate enough to include all physiological parameters, such as necrotic region radius and the hydraulic conductivity. Nevertheless, because the time scale of transport phenomena is much less than that of tumor growth, the physiological parameters can be considered time independent (Baxter & Jain, 1990).

We begin setting up the mathematical model by regarding the interstitium as an isotropic porous material, and describe the flow through the interstitium by Darcy's law (Scheidegger, 1963; Whitaker, 1986; Lowe & Barbenel, 1988; Bear, 1988; Huyghe, Arts, Van Campen, & Reneman, 1992), according to Equation 1:

$$u = k\nabla P_i \quad (1)$$

where:
k ($cm^2\ mm^{-1}\ Hg^{-1}\ s^{-1}$),
Pi ($mm\ Hg^{-1}$) and
u ($m\ s^{-1}$) are the hydraulic conductivity of the interstitium, the interstitial fluid pressure and the interstitial fluid velocity respectively (the Nomenclatures are listed in Appendix 1). There are some limitations to the use of Darcy's law. For instance, it is not applicable for non-Newtonian fluids, Newtonian fluids at high velocities, or for gases at very low or very high velocities. It is also shown that the friction within the fluid and exchange of momentum between the fluid and solid phases is neglected by Darcy's law. Fortunately, in the interstitium of biological tissues, all these exceptional cases are rare (most of the phenomena are low velocity for Newtonian fluids) except for the friction within the fluid; therefore, Darcy's law is quite applicable to the analysis of interstitial fluid flow.

The mass balance equation for a steady state incompressible fluid is that the divergence of the fluid flow is zero, or mathematically, according to Equation 2:

$$\nabla . u = 0 \quad (2)$$

Equation 2 is applicable in porous media. However, in tumors, sources and sinks are present. For example, between interstitial space and the blood vessels, fluid is exchanged; therefore, the steady state incompressible form of the continuity equation must be modified as Equation 3:

$$\nabla . u = \varphi_B - \varphi_L \quad (3)$$

Because there is no blood vessels in the necrotic region, we can rewrite Equation 3 as follows Equation 4:

$$\nabla . u = \begin{cases} \varphi_B - \varphi_L & \text{for } r \geq R_n \\ 0 & \text{for } r < R_n \end{cases} \quad (4)$$

where:
R_n (cm),
φ_B (s^{-1}) and
φ_L (s^{-1}) are the radius of the necrotic core, the fluid source term, and the lymphatic drainage term, respectively. There is no lymph vessels in a solid tumor and that means $\varphi_L = 0$.

The fluid source term is governed by Starling's law as follows Equation 5 (Starling, 1896):

$$\varphi_B = \frac{L_P S}{V}(P_b - P_i - \sigma_s(\pi_b - \pi_i)) \quad (5)$$

where:
S V^{-1} (cm^{-1}) is surface area per unit volume for transport in the tumor; L_p ($cm\ mm^{-1}\ Hg^{-1}\ s^{-1}$) hydraulic conductivity of the microvascular wall; P_b ($mm\ Hg^{-1}$) blood pressure, P_i ($mm\ Hg^{-1}$) interstitial pressure, σ_s ($mm\ Hg^{-1}$), average osmotic reflection coefficient for plasma proteins; π_b ($mm\ Hg^{-1}$), osmotic pressure of the plasma; and π_i ($mm\ Hg^{-1}$), osmotic pressure of the interstitial fluid.

Which the osmotic pressure contribution σ_s (π_b-π_i) is small (Stohrer, Boucher, Stangassinger, & Jain, 1995; 2000), Equation 5 reduces to Equation 6:

$$\varphi_B = \frac{L_P S}{V}(P_b - P_i) \quad (6)$$

Combination of Darcy's law and the continuity equation results in Equation 7 and 8:

$$-\nabla.\, k\nabla P_i = \varphi_B \quad (7)$$

$$-\nabla.\, k\nabla P_i = \frac{L_P S}{V}(P_b - P_i) \quad (8)$$

For necrotic region there is no blood vessels and so Equation 7 can be expressed by the very well-known Laplace Equation 9:

$$\nabla^2 P_i = 0 \quad (9)$$

In Equation 8 all parameters exept P_i and P_b are assumed constant, so Equation 8 can write as Equation 10:

$$\nabla^2 P_i = \frac{L_P S}{kV}(P_i - P_b) \quad (10)$$

In this study, we assume that interstitial fluid, flows in radial direction in cylindrical coordinate. In cylindrical coordinate Equation 10 can express as Equation 11:

$$\frac{1}{r}\frac{\partial}{\partial r}\left(r\frac{\partial p_i}{\partial r}\right) = \frac{L_P S}{kV}(P_i - P_b) \quad (11)$$

Applying the appropriate boundary conditions and also all the constants mentioned earlier, the governing equation, Equation 11 can be used to calculate the interstitial fluid velocity (IFV) and interstitial fluid pressure (IFP) profiles in solid tumors. For calculating IFP in Equation 11 we need to calculate blood pressure in capillaries.

The axial flow in a vessel (Q_b) follows Poiseuille's law with constant viscosity, (implicitly assumes steady, laminar flow with constant hematocrit and no shear rate dependence), according to Equation 12 (Pozrikidis, 2010):

$$Q_b = -\frac{\pi a^4}{8\mu}\frac{dP_b}{dz} \quad (12)$$

where:
μ is the blood viscosity, a is the capillary radius and P_b is the position dependent pressure inside the capillaries.

We assume that the extravasation flux of fluid from the vasculature into the surrounding interstitium is described by Starling's law, according to Equation 13 (Pozrikidis, 2010):

$$q_e = L_P[P_b(z) - P_i(r)] \quad (13)$$

Mass conservation for the fluid transported along a capillary requires (Pozrikidis, 2010), according to Equation 14:

$$\frac{dQ_b}{dz} + 2\pi a q_e(z) = 0 \quad (14)$$

Substituting Equation 12 and 13 into Equation 14 and rearranging, we have, according to Equation 15:

$$\frac{d^2 P_b}{dz^2} = \frac{16\mu L_P}{a^3}[P_b(z) - P_i(r)] \quad (15)$$

Now Equation 11 and 15 are used to obtain IFP and blood pressure. Applying the appropriate boundary conditions, due to symmetry, there is a no flux boundary condition at the center of the tumor; i.e., according to Equation 16:

$$\frac{\partial P_i}{\partial r}(r = 0) = 0 \quad (16)$$

At the outer edge of the solid tumor, r = R, the pressure in the surrounding tissue is fixed, and equal zero, according to Equation 17 (Baish et al., 1997).

$$P_i(r = R) = 0 \quad (17)$$

For blood pressure in capillaries, we have Equation 18:

$$P_b(z = 0) = P_{artery} \quad P_b(z = h) = P_{vein} \quad (18)$$

Now Equation 11 and 15 are coupled and appropriate boundary conditions are provided by Equation 16-18. To obtain interstitial and blood pressures, this two equation should be solved together. The solution now can be obtained analytically or numerically to find the IFV, IFP, blood pressure and velocity profiles for this condition. In this work, the numerical method has been used. A finite difference method (FDM) is applied to discretize the equations. The grids near the capillary wall are fine. In order to check the grid independency of the code, the results for three different grids are compared, indicating the conservative property of the numerical method. Final choice of the grid includes 12224 nodes.

Results and discussion

In order to validate the numerical method, the results of the paper are compared with Soltani and Chen (2011). In their work, the tumor is assumed as a sphere and blood flow in vessels has a constant pressure. The material properties (see Table 1) for tumor and normal tissue are considered the same as ones available in Soltani and Chen' study (2011).

Table 1. Material properties used in numerical simulations (Soltani & Chen, 2011).

Parameter	Tissue	Baseline value
k (cm^2 mm^{-1} Hg^{-1} s^{-1})	Normal	$8.53x10^{-9}$
	Tumor	$4.13x10^{-8}$
S V^{-1} (cm^{-1})	Normal	70
	Tumor	200
Lp (cm mm^{-1} Hg^{-1} s^{-1})	Normal	$0.36x10^{-7}$
	Tumor	$2.8x10^{-7}$
π_b(mm Hg^{-1})	Both	20
π_i (mm Hg^{-1})	Normal	10
	Tumor	15
σ_s(mm Hg^{-1})	Normal	0.91
	Tumor	0.82
P_b(mm Hg^{-1})	Both	15.6

For R = 1 cm in spherical tumor and properties in Table 1, IFP in tumor tissue is shown in Figure 2.

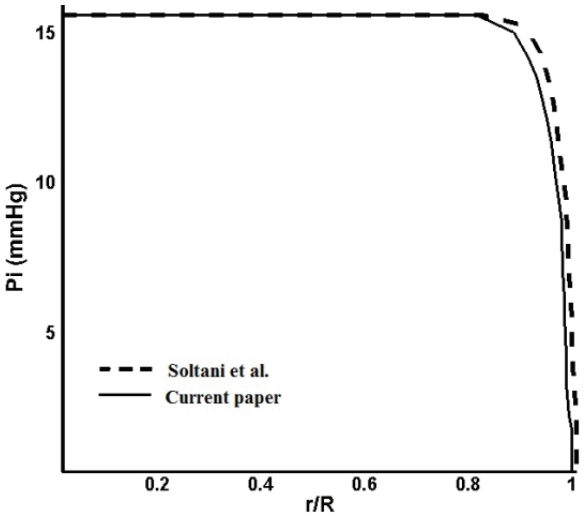

Figure 2. Interstitial pressure distribution in a spherical tumor with R = 1 cm.

For this paper, the tumor is assumed as a cylinder with constant radius and variable necrotic core and also variable intercapillary distance. Table 2 shows the parameters used in this paper.

In this paper we divide the tumor into three sections as it is shown in Figure 1:

- Section 1: the necrotic core,
- Section 2: the intercapillary space (the space between two capillaries),
- Section 3: the space between second capillary and tumor peripherical space.

Table 2. Properties used in this paper (Baish et al., 1997).

Parameter	value
k (cm^2 mm^{-1} Hg^{-1} s^{-1})	$2x10^{-7}$
S V^{-1} (cm^{-1})	200
Lp (cm mm^{-1} Hg^{-1} s^{-1})	$2.5x10^{-6}$
Arterial pressure (mm Hg^{-1})	15
μ (mm Hg-sec^{-1})	$3x10^{-5}$
Vessel diameter (μm)	15
Venous pressure (mm Hg^{-1})	10
Peripherical interstitial pressure (mm Hg^{-1})	0

Figure 3 shows the interstitial pressure distribution in a tumor with 0.4 cm necrotic core radius in z = 0 and in the necrotic core region (section1).

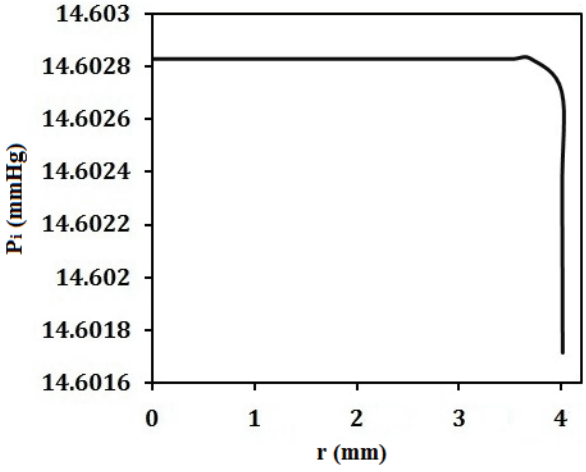

Figure 3. Interstitial pressure distribution in the necrotic core.

As it is shown in Figure 3, interstitial pressure has a constant value and near the first capillary it decreases.

Figure 4 shows the interstitial pressure distribution between two capillaries (intercapillary distance) (section 2). In this section, the IFP decreases rapidly. This figure shows that in the space between the capillaries, the interstitial fluid pressure profiles decreases with higher rate than near the capillaries. Figure 5 shows the interstitial pressure distribution after second capillary (section 3). In this section, IFP decreases until reaches to zero in the peripheral region of tumor.

For the first and second capillaries, the blood pressure are shown in Figure 6 and 7. Figure 8, 9 and 10 show the interstitial fluid velocity in the necrotic core (section 1), the intercapillary distance (section 2) and after the second capillary (section 3) respectively.

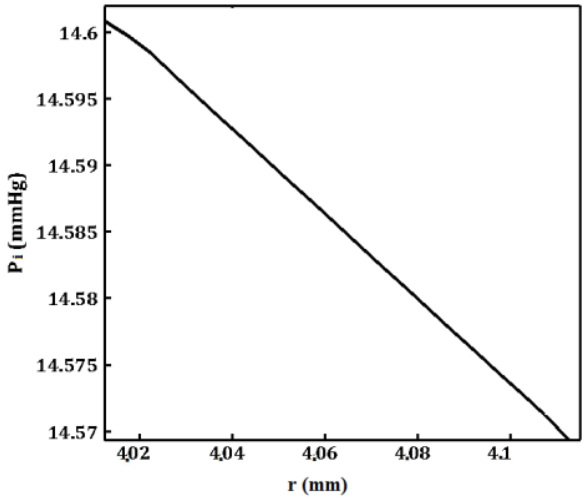

Figure 4. Interstitial pressure distribution in the intercapillary space.

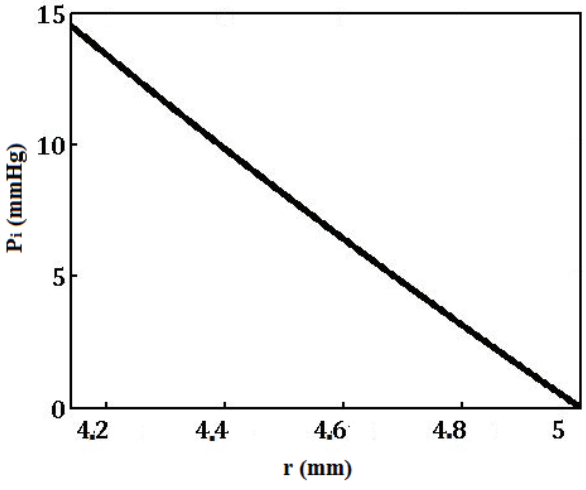

Figure 5. Interstitial pressure distribution after the second capillary.

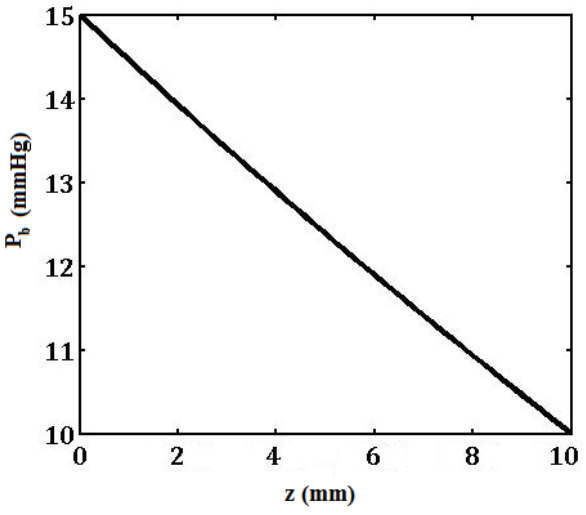

Figure 6. Blood pressure distribution in the fisrt capillary.

As it is shown in Figure 8, the interstitial fluid velocity in the necrotic region is zero and near the fisrt capillary it increases. In the intercapillary space, the interstitial fluid has more velocity magnitude than the necrotic core and finaly in Figure 10 the interstitial fluid has the most velocity magnitude. Blood velocity magnitude in the fisrt and second capillaries are the same and is shown in Figure 11. Figure 12 shows the interstitial pressure distribution in a 0.5 cm radius tumor, as a function of radius for different values of necrotic radii. This figure shows that an increase in the necrotic radius increases the maximum pressure inside the tumor. In this figure, the value of interstitial pressure is calculated from center of the tumor to second capillary (section 1 and 2).

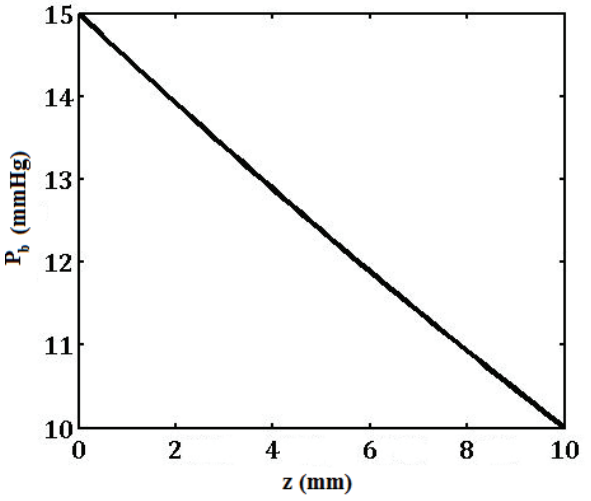

Figure 7. Blood pressure distribution in the second capillary.

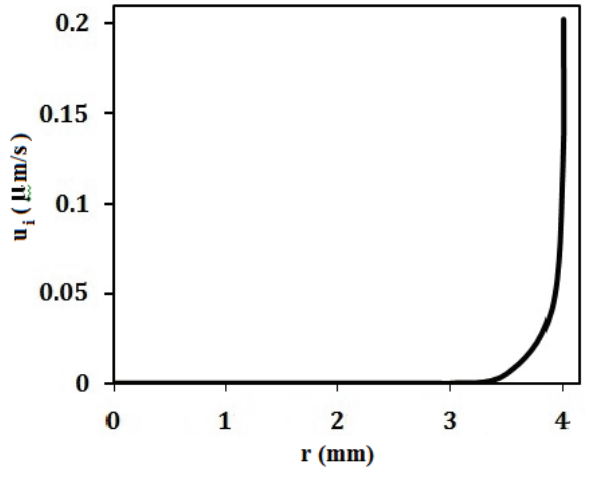

Figure 8. Interstitial fluid velocity in the necrotic core.

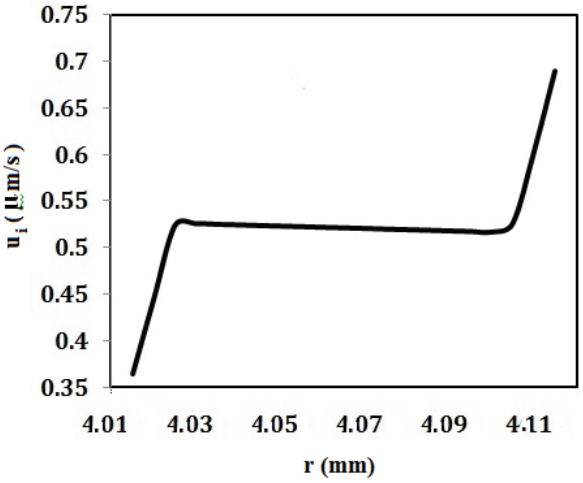

Figure 9. Interstitial fluid velocity in intercapillary space.

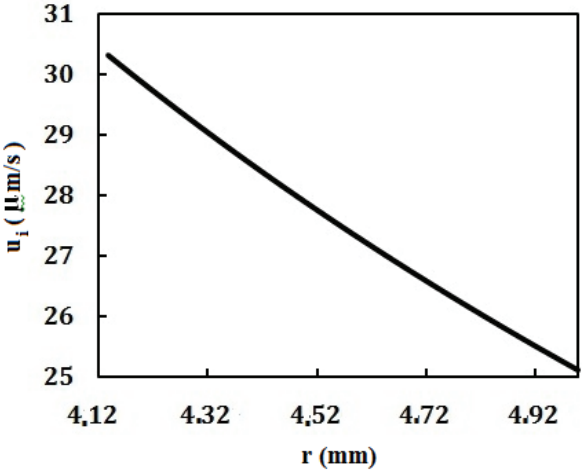

Figure 10. Interstitial fluid velocity after second capillary.

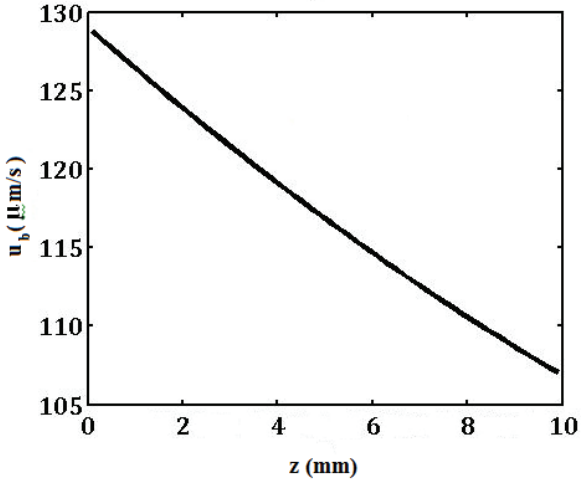

Figure 11. Blood velocity in the first and second capillaries.

Figure 13 shows the interstitial pressure distribution in whole tumor as a function of necrotic radius.

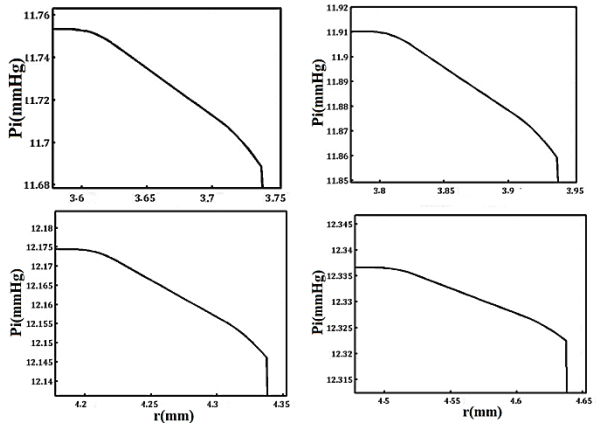

Figure 12. Interstitial pressure distribution from tumor center to second capillary at z = 5, a) R_n = 3.6, b) R_n = 3.8, c) R_n = 4.2, and d) R_n = 4.5 mm.

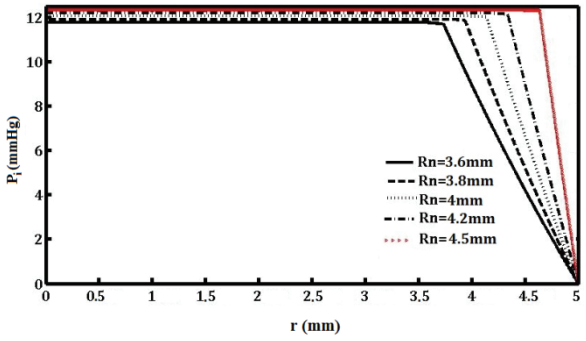

Figure 13. Interstitial pressure distribution as a function of necrotic radius at z = 5 mm.

Now in Figure 14, the intercapillary distance (named d) is changed in this geometry. In Figure 14 the interstitial pressure is calculated in section 1 and 2 due to the intercapillary distance changes. As it is shown, by increasing 'd' the IFP increases.

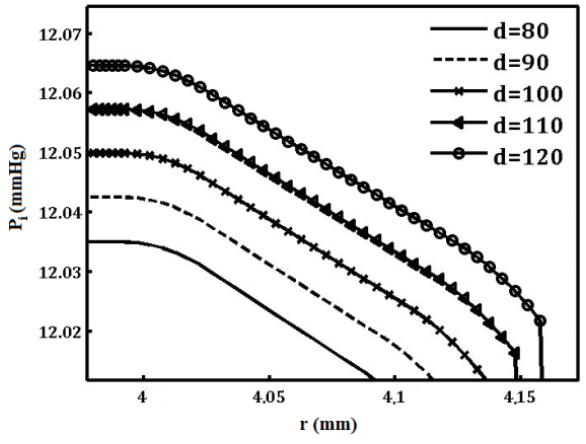

Figure 14. Interstitial pressure distribution as a function of intercapillry distance at z = 0 mm.

In Figure 15, the effect of geometrical parameters is considered. The surface area per unit volume for

transport in the tumor (S V^{-1}) is changed and result is shown in Figure 15. In this figure other parameters are: R_n = 4 mm, d = 120 μm and results is considered at z = 5 mm. Figure 16 shows the effect of hydraulic conductivity of the microvascular wall on the interstitial pressure distribution.

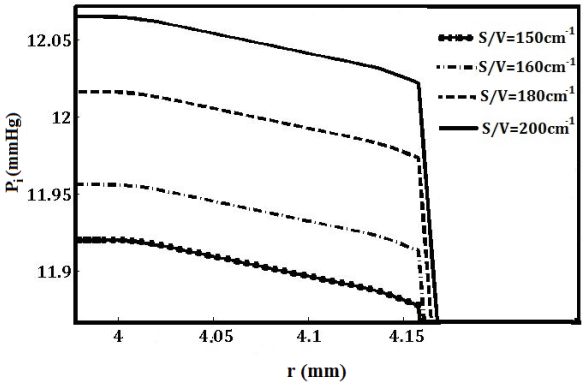

Figure 15. Interstitial pressure distribution as a function of S V^{-1}, at z = 5 mm.

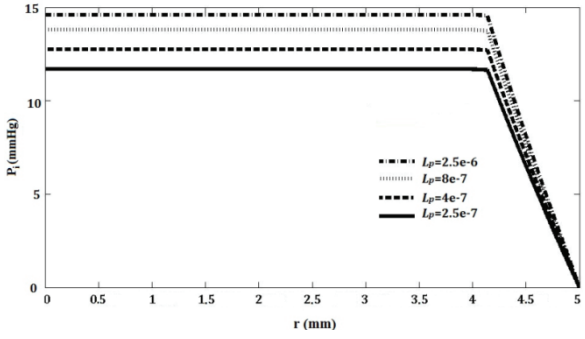

Figure 16. Interstitial pressure distribution as a function of L_p, at z = 5 mm.

Finally the IFP contribution in whole tumor, is shown in Figure 17. As it is mentioned, the IFP has maximum value in the necrotic core and by moving to the tumor peripheral space it decreases. Regardless of considering the Newtonian or NON-Newtonian assumptions, the pressure variation behavior inside the tumor is the same, which means that the maximum pressure always exists at tumor center and pressure decreases by moving toward the peripherical space. It should be mentioned that the values of the pressure for Newtonian and NON-Newtonian assumptions are not the same and this issue is now under investigation by authors.

Conclusion

A numerical solution is considered to calculate interstitial pressure in a cylindrical tumor with two capillaries and necrotic region. The results show that main cause of insufficient delivery of drugs is high interstitial pressure in the necrotic core. The main assumption used to draw this conclusion is that, drug particles flow with the interstitial fluid. The distribution of interstitial fluid pressure and velocity and pressure and velocity of blood, have been calculated by finite difference numerical method to the governing equations. Comparison of these numerical solutions and previous studies evidences the acuuracy of results.

Results show that the interstitial pressure has a maximum value at the center of the tumor and decreases towards the first capillary. This reduction continues in the region of between two capillaries and finally, interstitial pressure decreases toward the periphery of tumor. This study also shows that reduction in intercapillary distance may cause a decrease in the interstitial pressure and also changes in the necrotic radius can change the interstitial pressure.

In this study, interstitial and blood flow velocity distribution are considered. The results reveal that in the necrotic region, interstitial fluid velocity is zero and increases gradually and after second capillary, the interstitial fluid velocity decreases. Blood pressure and velocity have a quasi-linear changes.

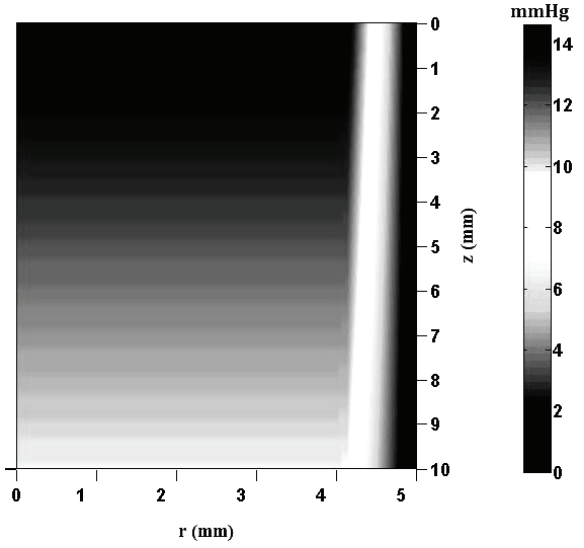

Figure 17. Interstitial pressure distribution in whole tumor.

Reference

Attaluri, A., Ma, R., Qiu, Y., Li, W., & Zhu, L. (2011). Nanoparticle distribution and temperature elevations in prostatic tumours in mice during magnetic nanoparticle hyperthermia. *International Journal of Hyperthermia, 27*(5), 491-502.

Baish, J. W., Netti, P. A., & Jain, R. K. (1997). Transmural coupling of fluid flow in microcirculatory network

and interstitium in tumors. *Microvascular Research, 53*(2), 128-141.

Baxter, L. T., & Jain, R. K. (1991a). Transport of fluid and macromolecules in tumors (III): role of binding and metabolism. *Microvascular Research, 41*(1), 5-23.

Baxter, L. T., & Jain, R. K. (1991b). Transport of fluid and macromolecules in tumors IV: a microscopic model of the perivascular distribution. *Microvascular Research, 41*(2), 252-272.

Baxter, L.T., & Jain, R. K. (1990). Transport of fluid and macromolecules in tumors (II): role of heterogeneous perfusion and lymphatics. *Microvascular Research, 40*(2), 246-263.

Bear, J. (1988). *Dynamics of fluids in porous media*. New York City, NY: Dover Publications.

Blakeslee, S. (1989). *Impenetrable tumors found to block even the newest cancer agents*. New York City, NY: The New York Times.

Goldacre, R. J., & Sylven, B. (1962). On the access of blood-borne dyes to various tumor regions. *British Journal of Cancer, 16*(2), 306-322.

Huyghe, J. M., Arts, T., Van Campen, D. H., & Reneman, R. S. (1992). Porous medium finite element model of the beating left ventricle. *American Journal of Physiology, 262*(4), 1256-1267.

Jain, R. K. (1988). Determinants of tumor blood flow: A review. *Cancer Research, 48*(10), 2641-2658.

Jain, R. K., & Baxter, L. T. (1988). Mechanisms of heterogeneous distribution of monoclonal antibodies and other macromolecules in tumors: significance of elevated interstitial pressure. *Cancer Research, 48*(24), 7022-7032.

Jain, R. K., & Hartley, K. W. (1984). Tumor blood flow-characterization, modifications, and role in hyperthermia. *IEEE Transactions on Sonics and Ultrasonics, 31*(5), 504-525.

Lowe, G. D. O., & Barbenel, J. C. (1988). Plasma and blood viscosity. In G. D. O. Lowe (Ed.), *Clinical blood rheology* (p. 11-24). Boca Raton, FL: CRC Press.

Matsuki, H., & Yanada, T. (1994). Temperature sensitive amorphous magnetic flakes for intra-tissue hyperthermia. *Materials Science and Engineering: A, 181-182*(1), 1366-1368.

McDougall, S. R., Anderson, A. R. A., Chaplain, M. A. J., & Sherratt, J. A. (2002). Mathematical modeling of flow through vascular network: implications for tumor-induced angiogenesis and chemotherapy strategies. *Bulletin of Mathematical Biology, 64*(4), 673-702.

Netti, P. A., Baxter, L. T., Boucher, Y., Skalak, R., & Jain, R. K. (1995). Time-dependent behavior of interstitial fluid pressure in solid tumors: implication for drug delivery. *Cancer Research, 55*(22), 5451-5458.

Powe, J., Pak, K. Y., Paik, C. H., Steplewski, Z., Ebbert, M. A., Herlyn, D., … Koprowski, H. (1984). Labeling monoclonal antibodies and F(ab')2 fragments with (111In) indium using cyclic DTPA anhydride and their in vivo behavior in mice bearing human tumor xenografts. *Cancer Drug Delivery, 1*(2), 125-135.

Pozrikidis, C. (2010). Numerical simulation of blood and interstitial flow through a solid tumor. *Journal of Mathematical Biology, 60*(1), 75-94.

Pozrikidis, C., & Farrow, D. A. (2003). A model of fluid flow in solid tumors. *Annals of Biomedical Engineering, 31*(2), 181-194.

Saltzman, W. M., & Radomsky, M. L. (1991). Drugs released from polymers: diffusion and elimination in brain tissue. *Chemical Engineering Science, 46*(10), 2429-2444.

Scheidegger, A. E. (1963). *The physics of flow through porous media*. Toronto, CA: University of Toronto Press.

Sefidgar, M., Soltani, M., Raahemifar, K., Bazmara, H., Nayinian, S. M. M., & Bazargan, M. (2014). Effect of tumor shape, size, and tissue transport properties on drug delivery to solid tumors. *Journal of Biological Engineering, 8*(12), 1-13.

Shah, S. A., Gallagher, B. M., & Sands, H. (1985). Radioimmuno detection of small human tumor xenografts in spleen of athymic mice by monoclonal antibodies. *Cancer Research, 45*(11), 5824-5829.

Soltani, M., & Chen, P. (2011). Numerical modeling of fluid flow in solid tumors. *PLoS One, 6*(6), 20344-20358.

Soltani, M., & Chen, P. (2012). Effect of tumor shape and size on drug delivery to solid tumors. *Journal of Biological Engineering, 6*(1), 4.

Starling, E. H. (1896). On the absorption of fluids from the connective tissue space. *The Journal of Physiology, 19*(4), 312-326.

Stohrer, M., Boucher, Y., Stangassinger, M., & Jain, R. K. (1995). *Oncotic pressure in human tumor xenografts* (86th ed.). Toronto, CA: Annual Meeting of the American Cancer Society.

Stohrer, M., Boucher, Y., Stangassinger, M., & Jain, R. K. (2000). Oncotic pressure in solid tumors is elevated. *Cancer Research, 60*(15), 4251-4255.

Wang, C. H., & Li, J. (1998). Three dimensional simulation of IgG delivery to tumors. *Chemical Engineering Science, 53*(20), 3579-3600.

Wang, C. H., Li, J., Teo, C. S., & Lee, T. (1999). The delivery of BCNU to brain tumors. *Journal of Controlled Release, 61*(1-2), 21-41.

Welter, M., & Rieger, H. (2013). Interstitial fluid flow and drug delivery in vascularized tumors: a computational model. *PLoS One, 8*(8), e70395.

Whitaker, S. (1986). Flow in porous media I: A theoretical derivation of Darcy's law. *Transport in Porous Media, 1*(1), 3-25.

Received on January 26, 2016.
Accepted on March 22, 2016.

The authors opted for the session results and discussion and only two bibliographic references.

Appendix 1. Nomenclatures.

k	Hydraulic conductivity
Pi	Interstitial fluid pressure
R_n	Necrotic core radious
φ_B	Fluid source term
φ_L	Lymphatic drainage term
L_p	Hydraulic conductivity
P_b	Blood pressure
σ_s	Average osmotic reflection coefficient
π_b	Osmotic pressure of the plasma
π_i	Osmotic pressure of the interstitial fluid
A	Capillary radius
μ	Blood viscosity
S	Tumor surface
V	Tumor volume